

Phase Equilibrium and Dielectric Relaxation in Mixture of 5CB with dilute Dimethyl Phthalate:
Effect of Coupling between Orientation and Composition Fluctuations on Molecular Dynamics
in Isotropic One-Phase State.

Ryoko Shimada,^{*a} Osamu Urakawa,^b Tadashi Inoue,^b and Hiroshi Watanabe^{*c}

^a*Department of Mathematical and Physical Sciences, Japan Women's University,
Bunkyo-ku, Tokyo 112-8681, Japan. E-mail: shimadar@fc.jwu.ac.jp*

^b*Department of Macromolecular Science, Faculty of Science, Osaka University,
Toyonaka, Osaka 560-0041, Japan.
E-mail: urakawa@chem.sci.osaka-u.ac.jp and tadashi@chem.sci.osaka-u.ac.jp*

^c*Institute for Chemical Research, Kyoto University
Uji, Kyoto 611-0011, Japan. E-mail: hiroshi@scl.kyoto-u.ac.jp*

*Corresponding authors

S1. Determination of composition in isotropic and nematic phases coexisting in DMP/5CB mixtures at $T < T_{IN}$.

Our visual observation (cf. Fig. 1 in the main text) clearly detected the phase changes in the DMP/5CB mixtures with T . Those changes were confirmed also from cross-polarized optical tests, as shown in Fig. S1 for the mixture with $w_{DMP} = 3.1$ wt%. The phase changes seen therein, from the isotropic one phase state at 28°C to the onset of phase separation into the isotropic and nematic phases at 27°C, and further to the nematic one phase state at $T = 25^\circ\text{C}$ -20°C (characterized by the nematic texture spread throughout the view field), well correspond to those noted in Fig. 1.

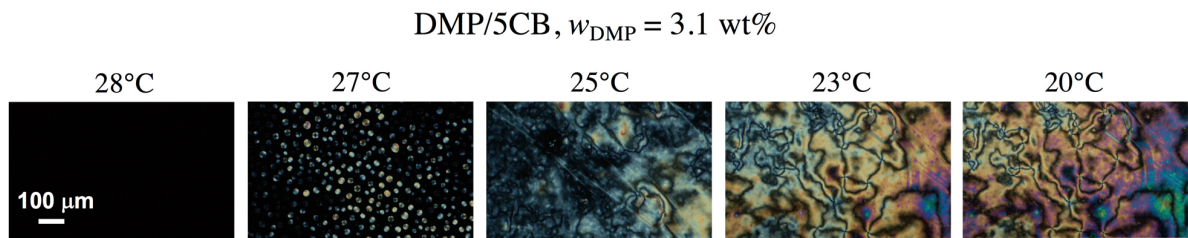


Fig. S1 Results of cross-polarized optical microscopy observation of DMP/5CB mixture ($w_{DMP} = 3.1$ wt%) at temperatures as indicated.

At temperatures where the DMP/5CB mixtures (charged in a glass flask; cf. Fig. 1) were separated into the isotropic and nematic phases, aliquots were taken from both phases and FTIR measurements were made for those aliquots diluted with chloroform. Fig. S2(a) shows an example of the IR adsorption coefficient A obtained for the isotropic and nematic phases (blue and red curves, respectively) coexisting at 22.0°C in a mixture having $w_{DMP, total} = 5.0$ wt %. (This mixture is DMP-rich compared to that examined in Fig. S1.) Logarithm of A is normalized at the wavenumber of 5CB adsorption (2228.3 cm^{-1}), so that the blue and red curves at wavenumbers $> 2200 \text{ cm}^{-1}$ are indistinguishable. On the basis of the Lambert-Beer law,¹ $\log A_{DMP}$ (at 1727.4 cm^{-1}) and $\log A_{5CB}$ (at 2228.3 cm^{-1}) exclusively assigned to adsorption of DMP and 5CB coexisting in the aliquot are related to each other as

$$\frac{\log A_{DMP}}{\log A_{5CB}} = K \frac{w_{DMP}}{1 - w_{DMP}} \quad \text{with} \quad K = \frac{\{\epsilon_{DMP} / M_{DMP}\}}{\{\epsilon_{5CB} / M_{5CB}\}} \quad (= 5.8) \quad (\text{S1})$$

Here, w_{DMP} is the DMP weight fraction in the aliquot, ϵ_{DMP} and ϵ_{5CB} are the molar adsorption coefficients of DMP and 5CB at respective adsorption bands, and M_{DMP} and M_{5CB} are respective molecular weights. Calibration with DMP/5CB mixtures having known w_{DMP} (Fig. S2(b)) showed that the $\log A_{DMP} / \log A_{5CB}$ ratio was indeed proportional to a $w_{DMP} / (1 - w_{DMP})$ factor (cf. eq S1) and gave the value of the pre-factor $K (= 5.8)$. This K value was utilized to determine w_{DMP} in the

isotropic and nematic phases coexisting in the DMP/5CB mixture. The results are summarized as the phase diagram (Fig. 3 in the main text).

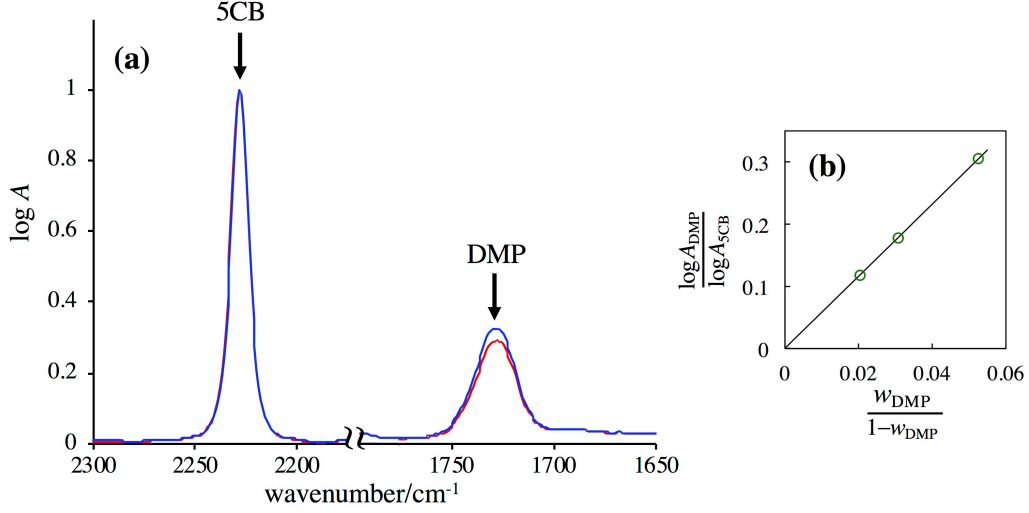


Fig. S2 (a) IR adsorption coefficient A of aliquots taken from isotropic and nematic phases (blue and red curves, respectively) of DMP/5CB mixture ($w_{\text{DMP, total}} = 5.0$ wt%) coexisting at 22.0°C . (b) Calibration of A obtained from mixtures having known w_{DMP} .

S2. Analysis of free energy given by simple model.

For the DMP/5CB mixture, the current study adopts the simplest possible expression of the free energy G contributed from the Flory-Huggins type mixing entropy² and the Landau-de Gennes (LdG) type nematic interaction³ (cf. eqs 4-6 in the main text),

$$\begin{aligned} \frac{G_\theta}{RT} = & n_{0,\theta} \ln \phi_{0,\theta} + n_{1,\theta} \ln \phi_{1,\theta} \\ & + n_{1,\theta} \left\{ A(\phi_{0,\theta}) \left[T - T^{**}(\phi_{0,\theta}) \right] Q_\theta^2 + B(\phi_{0,\theta}) Q_\theta^3 + C(\phi_{0,\theta}) Q_\theta^4 \right\} \end{aligned} \quad (\text{S2})$$

The subscript θ specifies the phase in the DMP/5CB mixture, $n_{0,\theta}$ and $n_{1,\theta}$ denote the mole numbers of DMP (component 0) and 5CB (component 1) in the phase θ , and $\phi_{0,\theta}$ and $\phi_{1,\theta}$ are the volume fractions of DMP and 5CB in the phase θ . Q_θ is the scalar orientational order parameter of 5CB in the phase θ , and A , B , C , and T^{**} are phenomenological LdG parameters that depend, in principle, on $\phi_{0,\theta}$. Eq. S2 can be analyzed straightforwardly to give the DMP volume fractions in the coexisting isotropic and nematic phases in the mixture at equilibrium, as explained below.

Hereafter, the indices α and β (instead of θ) are used to exclusively designate the nematic and isotropic phases (*i.e.*, $Q_\alpha > 0$ and $Q_\beta = 0$), respectively. We start with the equilibrium condition with respect to the orientational order parameter Q_α in the phase α , $(\partial\{G_\alpha + G_\beta\}/\partial Q_\alpha)_{n_{0,\alpha}, n_{1,\alpha}, Q_\beta(=0)} = 0$ (eq 9a in the main text). We apply this condition to the total free energy $\{G_\alpha + G_\beta\}$ specified by eq S2 to find

$$\left\{2A(\phi_{0,\alpha})\left[T - T^{**}(\phi_{0,\alpha})\right] + 3B(\phi_{0,\alpha})Q_\alpha + 4C(\phi_{0,\alpha})Q_\alpha^2\right\}Q_\alpha = 0 \quad (\text{S3})$$

Eq S3 has the following solution $Q_\alpha(\phi_{0,\alpha}) > 0$,

$$Q_\alpha(\phi_{0,\alpha}) = \frac{1}{8C(\phi_{0,\alpha})} \left\{ -3B(\phi_{0,\alpha}) + \sqrt{J_\alpha(\phi_{0,\alpha})} \right\} \quad (\text{S4})$$

with

$$J_\alpha(\phi_{0,\alpha}) \equiv 9B(\phi_{0,\alpha})^2 - 32A(\phi_{0,\alpha})\left\{T - T^{**}(\phi_{0,\alpha})\right\}C(\phi_{0,\alpha}) \quad (\text{S5})$$

given that $J_\alpha(\phi_{0,\alpha}) > 0$. Furthermore, the nematic phase having this $Q_\alpha(\phi_{0,\alpha})$ is stable if the following condition (deduced from eqs 4-6 and 9b in the main text) is satisfied.

$$P_\alpha(\phi_{0,\alpha}) \equiv -3B(\phi_{0,\alpha})Q_\alpha(\phi_{0,\alpha}) - 4A(\phi_{0,\alpha})\left[T - T^{**}(\phi_{0,\alpha})\right] > 0 \quad (\text{S6})$$

In fact, the numerical calculation explained later showed that $J_\alpha > 0$ and $P_\alpha > 0$ at low T thereby giving $Q_\alpha(\phi_{0,\alpha}) > 0$ (eq S4) as a stable solution of eq S3. In contrast, at high T , the solution $Q_\alpha(\phi_{0,\alpha}) > 0$ vanished and the mixture was in the isotropic one-phase state.

Now, we focus on the equilibrium condition with respect to the mole number $n_{j,\alpha}$ of the component j ($= 0, 1$) in the phase α , $(\partial\{G_\alpha + G_\beta\} / \partial n_{j,\alpha})_{n_{i,\alpha}(i \neq j), Q_\alpha, Q_\beta (=0)} = 0$; cf. eq 8a in the main text. Applying this condition to the total free energy $\{G_\alpha + G_\beta\}$ specified by eq S2 and considering relationships derived from eq 7 in the main text, $(\partial\phi_0 / \partial n_0)_{n_1} = -(\partial\phi_1 / \partial n_0)_{n_1} = (1 - \phi_0) / (n_0 + N_1 n_1)$ and $(\partial\phi_0 / \partial n_1)_{n_0} = -(\partial\phi_1 / \partial n_1)_{n_0} = -N_1 \phi_0 / (n_0 + N_1 n_1)$ with N_1 ($\cong 2$) being the molar volume ratio of 5CB to DMP, we find relationships among the DMP volume fractions $\phi_{0,\alpha}$ and $\phi_{0,\beta}$ in the nematic and isotropic phases α and β and the orientational order parameter Q_α in the phase α as

$$\ln\phi_{0,\alpha} - \ln\phi_{0,\beta} + \left(1 - \frac{1}{N_1}\right)(\phi_{0,\beta} - \phi_{0,\alpha}) = -Q_\alpha^2 \frac{(1 - \phi_{0,\alpha})^2}{N_1} L(\phi_{0,\alpha}, Q_\alpha; T) \quad (\text{S7})$$

$$\begin{aligned} & \ln(1 - \phi_{0,\alpha}) - \ln(1 - \phi_{0,\beta}) + (1 - N_1)(\phi_{0,\alpha} - \phi_{0,\beta}) \\ & = Q_\alpha^2 \left\{ \phi_{0,\alpha} (1 - \phi_{0,\alpha}) L(\phi_{0,\alpha}, Q_\alpha; T) - A(T - T^{**}) - BQ_\alpha - CQ_\alpha^2 \right\} \end{aligned} \quad (\text{S8})$$

with

$$L(\phi_{0,\alpha}, Q_\alpha; T) = \frac{d\left\{A(\phi_{0,\alpha})\left[T - T^{**}(\phi_{0,\alpha})\right]\right\}}{d\phi_{0,\alpha}} + Q_\alpha \frac{dB(\phi_{0,\alpha})}{d\phi_{0,\alpha}} + Q_\alpha^2 \frac{dC(\phi_{0,\alpha})}{d\phi_{0,\alpha}} \quad (\text{S9})$$

(Q_α and the LdG parameters A , B , C , and T^{**} are dependent on $\phi_{0,\alpha}$, but this dependence is not explicitly shown in eqs S7-S9 so as to avoid complication/confusion in these equations.) Eqs S7 and

S8 give $\phi_{0,\alpha} = \phi_{0,\beta}$ (no phase separation) if $Q_\alpha = 0$, which confirms that the isotropic-to-nematic transition of 5CB triggers the phase separation in the DMP/5CB mixtures.

Because the DMP volume fractions $\phi_{0,\alpha}$ and $\phi_{0,\beta}$ in our DMP/5CB mixtures are considerably small (≤ 0.05 ; cf. Fig. 3 in the main text), we can replace the terms $\ln(1-\phi_0)$ appearing in eq S8 by $-(\phi_0 + \phi_0^2/2)$ with a negligibly small error. Then, eq S8 reduces to a simple quadratic equation for a difference $\Delta\phi = \phi_{0,\beta} - \phi_{0,\alpha}$,

$$\Delta\phi^2 + 2\left\{\phi_{0,\alpha} + N_1\right\}\Delta\phi + 2Q_\alpha^2 h(\phi_{0,\alpha}, Q_\alpha; T) = 0 \quad (\text{S10})$$

with

$$h(\phi_{0,\alpha}, Q_\alpha; T) = A(T - T^{**}) + BQ_\alpha + CQ_\alpha^2 - \phi_{0,\alpha}(1 - \phi_{0,\alpha})L(\phi_{0,\alpha}, Q_\alpha; T) \quad (< 0) \quad (\text{S11})$$

where $L(\phi_{0,\alpha}, Q_\alpha; T)$ is given by eq S9. From eq S10, $\Delta\phi$ is obtained as

$$\Delta\phi = \sqrt{\left\{N_1 + \phi_{0,\alpha}\right\}^2 - 2Q_\alpha^2 h(\phi_{0,\alpha}, Q_\alpha; T) - \left\{N_1 + \phi_{0,\alpha}\right\}} \quad (> 0) \quad (\text{S12})$$

Replacing $\phi_{0,\beta}$ in eq S7 by $\phi_{0,\alpha} + \Delta\phi$, we obtain the following equation that determines $\phi_{0,\alpha}$ (in the nematic phase) as a function of the temperature T .

$$\ln\left(\frac{\phi_{0,\alpha}}{\phi_{0,\alpha} + \Delta\phi}\right) + \left(1 - \frac{1}{N_1}\right)\Delta\phi + \frac{(1 - \phi_{0,\alpha})^2}{N_1}Q_\alpha^2 L(\phi_{0,\alpha}, Q_\alpha; T) = 0 \quad (\text{S13})$$

If functional forms ($\phi_{0,\alpha}$ dependence) of the LdG parameters $A(\phi_{0,\alpha})$, $B(\phi_{0,\alpha})$, $C(\phi_{0,\alpha})$, and $T^{**}(\phi_{0,\alpha})$ are known, $Q_\alpha(\phi_{0,\alpha})$ is explicitly expressed as a function of $\phi_{0,\alpha}$ and T (cf. eq S4). Furthermore, we can utilize this $Q_\alpha(\phi_{0,\alpha})$ to explicitly express $L(\phi_{0,\alpha}, Q_\alpha; T)$ (eq S9), $h(\phi_{0,\alpha}, Q_\alpha; T)$ (eq S11), and $\Delta\phi$ (eq S12) as functions of $\phi_{0,\alpha}$ and T . Then, eq S13 includes just $\phi_{0,\alpha}$ and T as variables, which allows us to numerically calculate $\phi_{0,\alpha}$ for a given T . Actually, we assumed simple functional forms for $A(\phi_{0,\alpha})$, $B(\phi_{0,\alpha})$, $C(\phi_{0,\alpha})$, and $T^{**}(\phi_{0,\alpha})$ to conduct this numerical calculation, as explained below.

For our DMP/5CB mixtures having small $\phi_{0,\alpha}$ (≤ 0.05), we can safely assume first-order Maclaurin expansion forms for those LdG parameters specified by the following equations (identical to eqs 10a-10d in the main text).

$$A(\phi_{0,\alpha}) = A^\circ + A'\phi_{0,\alpha} \quad (> 0) \quad (\text{S14a})$$

$$B(\phi_{0,\alpha}) = B^\circ + B'\phi_{0,\alpha} \quad (< 0) \quad (\text{S14b})$$

$$C(\phi_{0,\alpha}) = C^\circ + C'\phi_{0,\alpha} \quad (> 0) \quad (\text{S14c})$$

$$T^{**}(\phi_{0,\alpha}) = T_{\text{IN}}^\circ + T'\phi_{0,\alpha} \quad (T' < 0) \quad (\text{S14d})$$

Then, $Q_\alpha(\phi_{0,\alpha})$, $L(\phi_{0,\alpha}, Q_\alpha; T)$, $h(\phi_{0,\alpha}, Q_\alpha; T)$, and $\Delta\phi$ are explicitly expressed as functions of $\phi_{0,\alpha}$ and T (cf. eqs S4, S9, S11, and S12), with the parameters in eqs S14a-S14d ($A^\circ, A', B^\circ, B', C^\circ, C', T_{\text{IN}}^\circ$, and T') being included as numerical coefficients in these functions. We utilized those functions in eq S13 to numerically calculate $\phi_{0,\alpha}$ for a given temperature T . Specifically, we scanned $\phi_{0,\alpha}$ in a range between 0 and 1 to find the $\phi_{0,\alpha}$ value that satisfied eq S13 for the given T . An example of this numerical calculation is shown in Fig. S3 where the left-hand-side of eq S13 calculated for $T = 24.0^\circ\text{C}$ is shown with the red curve. The expansion parameters utilized in the calculation are summarized in Table 2 in the main text. The value of $\phi_{0,\alpha} = 0.03294$ satisfies eq S13, as noted for the crossing of the red curve and horizontal dotted line. The corresponding $\Delta\phi (= 0.00217$; cf. eq S12) gives $\phi_{0,\beta} = \phi_{0,\alpha} + \Delta\phi = 0.03511$. These $\phi_{0,\alpha}$ and $\phi_{0,\beta}(T)$ values were confirmed to satisfy the stability conditions, eqs 8b and 9b in the main text.

The $\phi_{0,\alpha}$ and $\phi_{0,\beta}$ values determined as above were dependent on T , thereby specifying the transition temperatures deduced from our model. Namely, $T_{\text{IN}} = T$ and $T_{\text{IN}}^* = T$ for the DMP volume fractions $\phi_{0,\beta}(T)$ and $\phi_{0,\alpha}(T)$ in the isotropic and nematic phases coexisting at the temperature T . These T_{IN} and T_{IN}^* deduced from our model are shown in Fig. 3 in the main text with the red and blue curves.

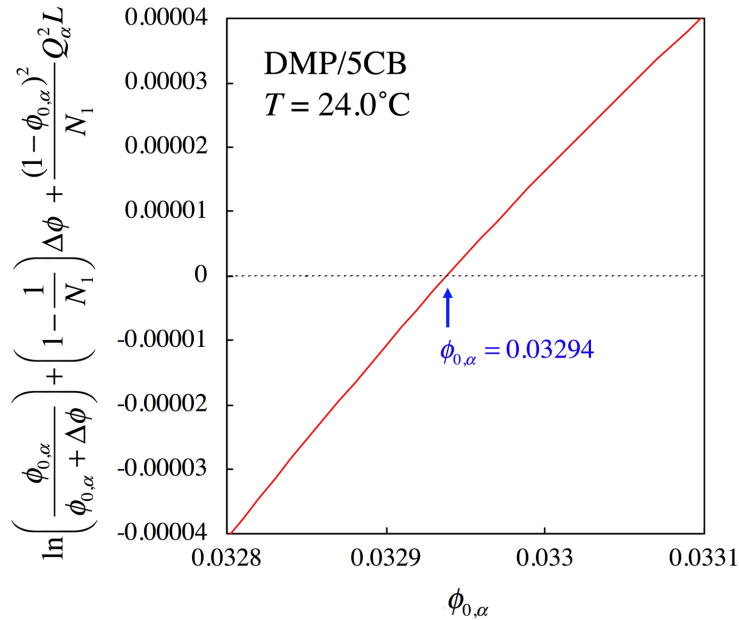


Fig. S3 Numerical determination of the DMP volume fraction $\phi_{0,\alpha}$ in the nematic phase of DMP/5CB mixture at 24.0°C deduced from our model. The left-hand-side of eq S13 (calculated from the parameters summarized in Table 2 in the main text) is plotted against $\phi_{0,\alpha}$; see red curve.

S3. Dielectric Behavior of pure DMP.

Fig. S4 shows the ε'' data of pure DMP at representative temperatures as indicated. Intensive dielectric relaxation noted for those data reflects rotational motion of DMP molecules (having a large dipole due to the $-\text{COO}$ group). The data obey the time-temperature superposition, except at their low- ω tail, as shown in Fig. S5. (The DMP molecules might exhibit T -dependent collective dynamics to have this low- ω tail, although its detail is still unclear.)

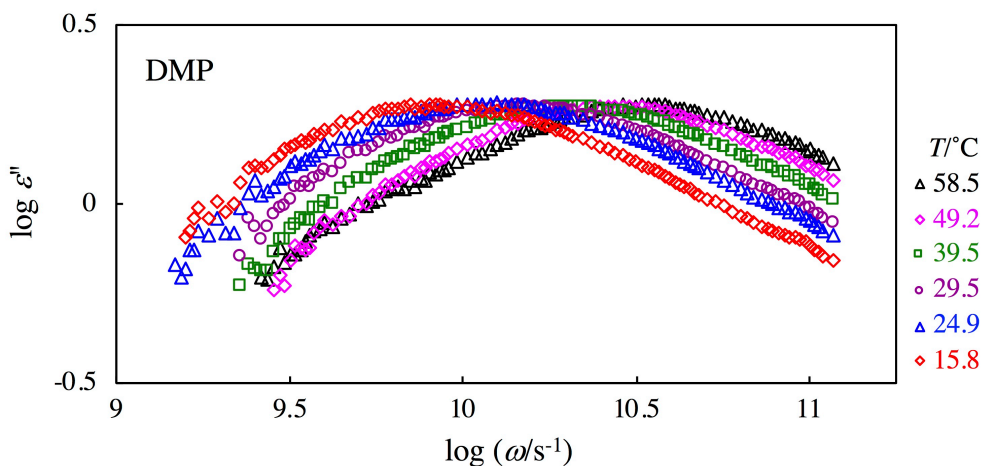


Fig. S4 ε'' data of pure DMP at temperatures as indicated.

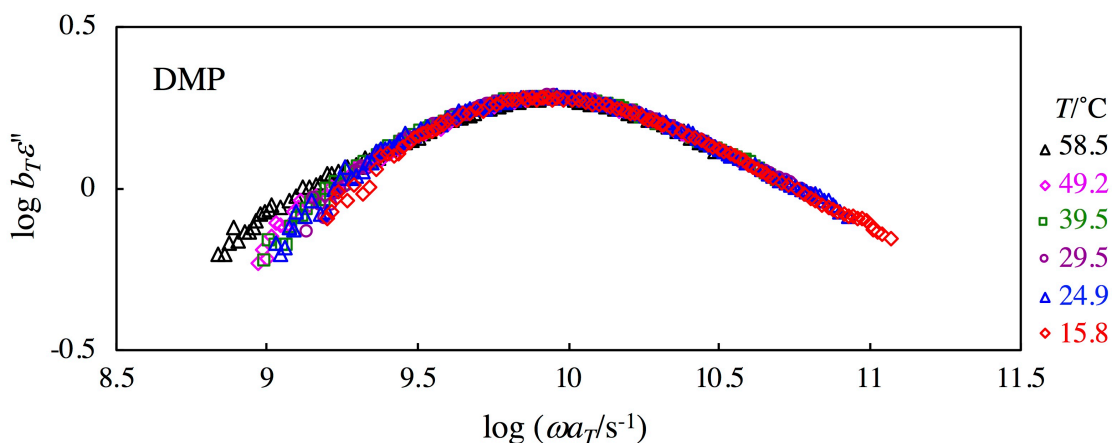


Fig. S5 Test of time-temperature superposition for ε'' data of pure DMP. Data are reduced at $T_r = 15.8^\circ\text{C}$.

In Fig. S6, the dielectric relaxation time evaluated from the angular frequency at the ε'' -peak, $\tau_\varepsilon = 1/\omega_{\text{peak}}$, is compared for pure DMP and DMP/5CB mixture ($w_{\text{DMP}} = 3.1 \text{ wt}\%$). In the entire range of T , τ_ε is much larger (by a factor > 100) for the mixture than for pure DMP. This result strongly suggests that the dielectric relaxation of the mixture, seen in Fig. 5 in the main text, detects the rotational dynamics of 5CB molecules (the major component therein).

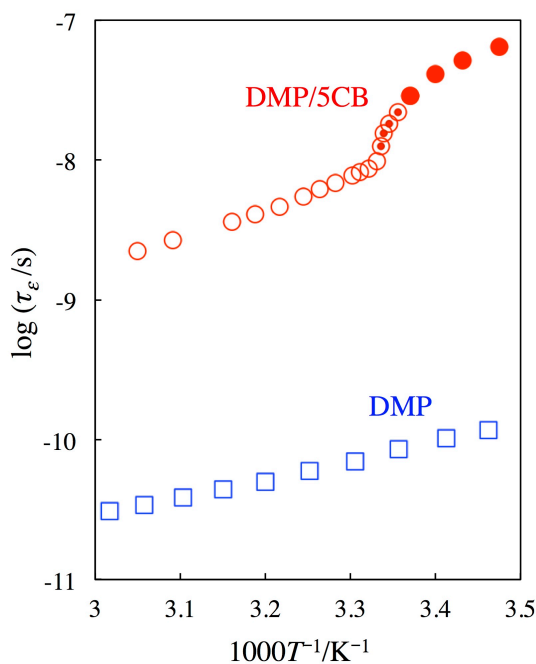


Fig. S6 Comparison of dielectric relaxation times of pure DMP and DMP/5CB mixture ($w_{\text{DMP}} = 3.1 \text{ wt}\%$).

S4. Relaxation mode distribution of pure 5CB and DMP/5CB mixture.

Fig. S7 tests validity of the time-temperature superposition for the ϵ'' data of pure 5CB. The superposition works well at T higher than the isotropic-to-nematic transition temperature T_{IN}° ($\cong 35.0^{\circ}\text{C}$) by 2.9°C or more; cf. Fig. S7(a). Thus, the dielectric mode distribution of pure 5CB broadens and the superposition fails only when T is decreased to the close vicinity of T_{IN}° , as noted from comparison of the data at 35.4 and 35.2°C (colored symbols in Figs. S7(b)) and at $T > T_{\text{IN}}^{\circ} + 2.9^{\circ}\text{C}$ (black symbols therein). The broadening seen for the colored symbols can be related to the orientation fluctuation coupled with the density fluctuation in this vicinity of T_{IN}° , as discussed in the main text.

In contrast, at T well below T_{IN}° where the nematic texture is developed, the mode distribution becomes bimodal; cf. colored symbols in Fig. S7(c). This bimodal distribution, most clearly noted for a high- ω hump of the ϵ'' curve at 26.3°C , reflects a difference in the dielectrically detected rotational motion of 5CB molecules for two cases the nematic director being parallel and perpendicular to the electric field utilized in the measurement,^{4,7} as explained in the main text. (This difference is most clearly noted when the director is macroscopically aligned under a magnetic field and/or shear.^{4,7}) Even at such low T , the terminal peak at $\omega < \omega_{\text{peak}}$ remains as sharp as the Debye (single-Maxwellian) peak shown with the dotted black curve. In fact, this sharpness of the terminal peak is noted at all T examined.

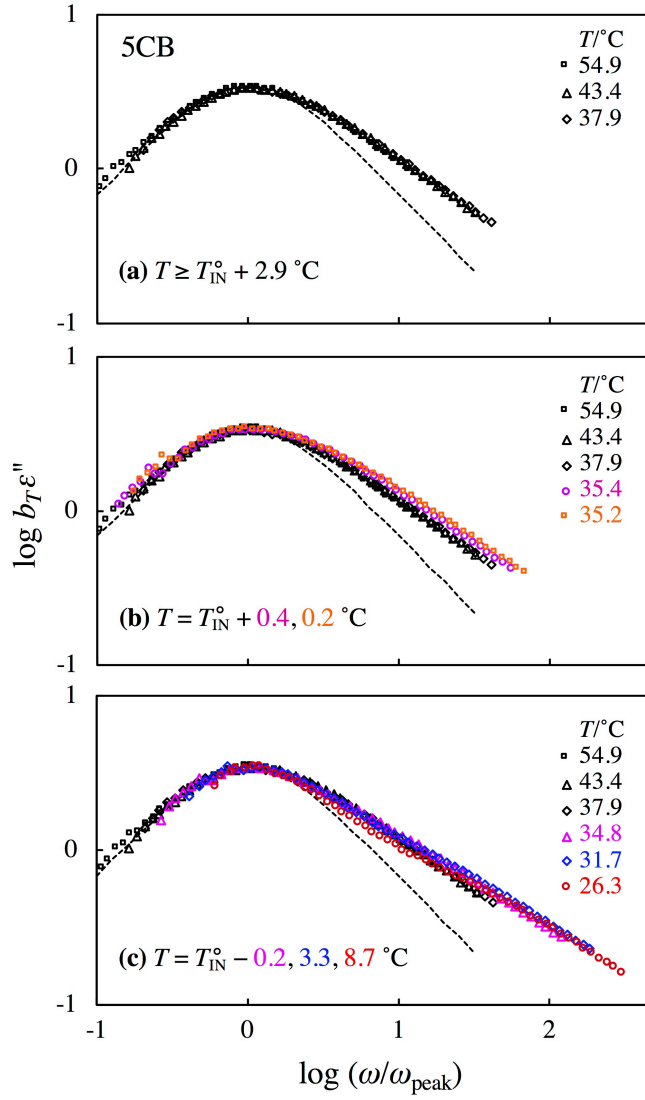


Fig. S7 Test of time-temperature superposition for ε'' data of pure 5CB. Data are plotted against $\omega/\omega_{\text{peak}}$.

Fig. S8 presents results of the same test for the DMP/5CB mixture ($w_{\text{DMP}} = 3.1$ wt%). The time-temperature superposition works well only at T higher than $T_{\text{IN}} (\cong 27.0$ °C) by 10.9 °C or more (Fig. S8(a)), and it fails in a wide range of T between T_{IN} and $T_{\text{IN}} + 10.9$ °C (cf. colored symbols in Fig. S8(b)). This failure, seen for the mixture in the *isotropic one-phase state*, should reflect coupling of the orientation and composition fluctuations occurring in this range of T (that is much wider than the range for the coupling of the orientation and density fluctuations noted for pure 5CB; cf. Fig. S7(b)).

The mode broadening of the mixture proceeds on a decrease of T below T_{IN} (cf. Fig. S8(c)) and further below $T_{\text{IN}}^* (\cong 25.0$ °C; cf. Fig. S8(d)). This broadening can be related to the coexistence of the 5CB molecules in the isotropic and nematic phases (at T between T_{IN} and T_{IN}^*), and also to a difference of the rotational motion of 5CB molecules in different directions with respect to the nematic director and the electric field (at $T < T_{\text{IN}}^*$) as explained above for the pure 5CB system. Nevertheless, the terminal peak at $\omega < \omega_{\text{peak}}$ remains as sharp as the Debye peak (dotted black curve) in the entire range of T , as similar to the behavior of pure 5CB.

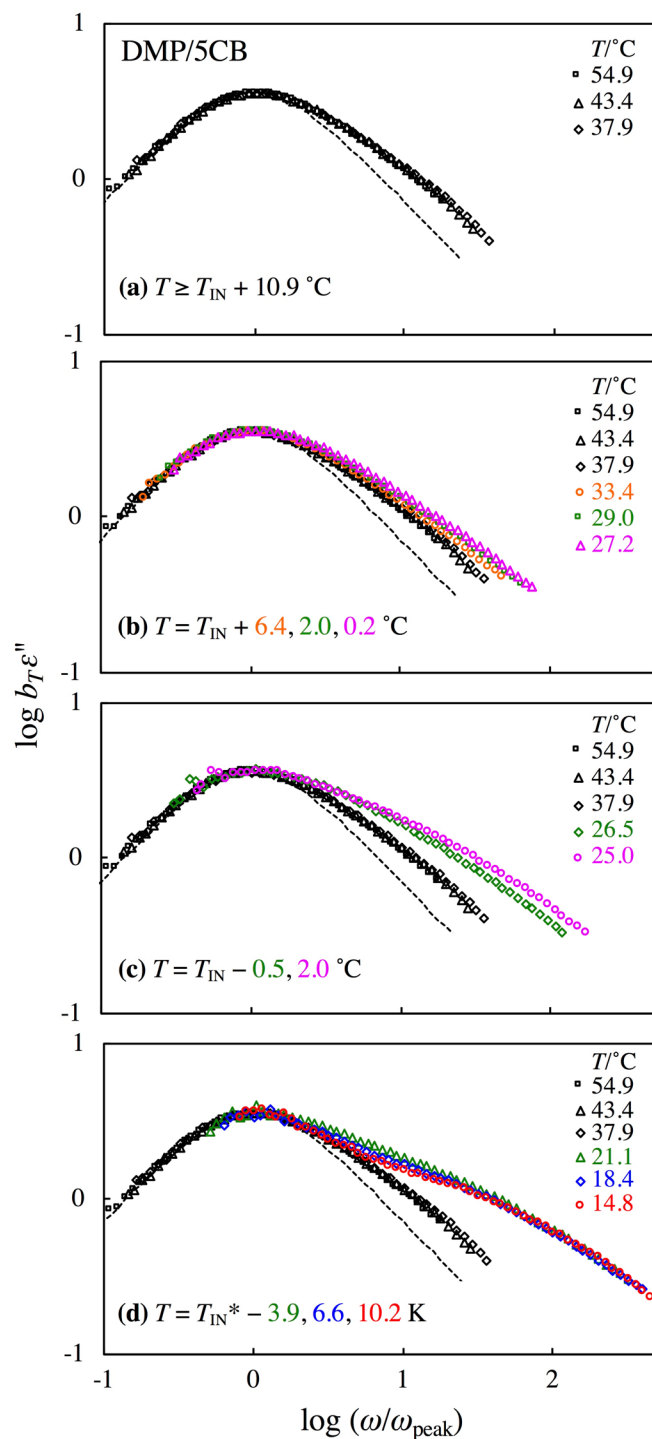


Fig. S8 Test of time-temperature superposition for ε'' data of DMP/5CB mixture ($w_{\text{DMP}} = 3.1$ wt%). Data are plotted against $\omega/\omega_{\text{peak}}$.

References

- 1) P. Atkins and J. de Paula, *Physical Chemistry*, 8th Ed., Oxford University Press, New York, Chapter 13, 2006.
- 2) M. Rubinstein and R. H. Colby, *Polymer Physics*, Oxford University Press, New York, 2003.
- 3) P. G. de Gennes and J. Prost, *The Physics of Liquid Crystals*, 2nd Ed, Clarendon Press, Oxford, 1993.
- 4) M. Davies, R. Moutran, A. H. Price, M. S. Beevers, and G. Williams, *J. Chem. Soc. Faraday II*, 1976, **72**,1447.
- 5) D. Lippens, J. P. Parneix, and A. Chapoton, *J. de Physique*, 1977, **38**,1465.
- 6) W. H. de Jeu, *Physical Properties of Liquid Crystalline Materials*, Gordon and Breach Science Publishers, New York, 1980.
- 7) H. Watanabe, T. Sato, M. Hirose, K. Osaki, and M.-L. Yao, *Rheol. Acta*, 1998, **37**, 519.